

Molecular Ordering and Adsorbate Induced Faceting in the Ag{110}–(S)-Glutamic Acid System

T. E. Jones and C. J. Baddeley*

EaStCHEM School of Chemistry, University of St Andrews, St Andrews, Fife, United Kingdom KY16 9ST

A. Gerbi, L. Savio, M. Rocca, and L. Vattuone

IMEM-CNR and CNISM, Dipartimento di Fisica, Università di Genova, Via Dodecaneso 33-16146 Genova, Italia

Received February 15, 2005. In Final Form: July 22, 2005

The adsorption of the amino acid, (S)-glutamic acid, was investigated on Ag{110} as a function of coverage and adsorption temperature using the techniques of scanning tunneling microscopy, low energy electron diffraction, and reflection absorption infrared spectroscopy. In the monolayer, (S)-glutamic acid was found to adsorb predominantly in the anionic glutamate form. Several discrete ordered adlayer structures were observed depending on preparation conditions. In addition, (S)-glutamic acid was found to induce both one- and two-dimensional faceting of the Ag{110} surface. In some cases, evidence was found that the 2-D faceting involved the creation of a chiral facet distribution. A comparison is made of the Ag/(S)-glutamic acid system with analogous studies of amino acids on Cu.

Introduction

In the past decade, there has been increasing interest in the interaction of simple amino acids with metal surfaces. These molecules represent model systems for chemisorption of biofunctional molecules and as stepping stones toward elucidating the important and complex interactions of peptides and proteins with surfaces. Protein interactions are important in issues of biocompatibility; in cell-surface interactions and in the development of technologies such as biosensors.

To date most work has concentrated on the adsorption of the simplest amino acids, glycine,^{1–13} alanine,^{14,15} phenylalanine,¹⁶ lysine,^{17,18} and aspartic acid,¹⁹ on various

crystal faces of copper. In general, these systems display ordered adlayer structures with the dominant chemisorbed species being the anionic form ($\text{H}_2\text{N.CR}^-\text{R}''.\text{COO}^-$, where R represents some functional group, e.g., H, CH_2 , C_6H_5 , etc.). On copper, there is also a strong tendency for adsorbate induced faceting of the surface as demonstrated for aminobenzoic acid on Cu{110}²⁰ and lysine on Cu{100}.¹⁷ The study of amino acid adsorption on silver is less extensive. Stewart and Fredericks²¹ studied the adsorption of amino acids on roughened silver surfaces with SERS and concluded that glutamate (and the other amino acids) adsorbs in the zwitterionic form at room temperature. Zhao²² reported that glycine was unable to chemisorb to Ag at 300 K. In addition, Zhao et al. reported that glycine physisorbs on Au{110}–(1 × 2) and induces various reconstructions of the Au surfaces.²³ Zhao's definition of a physisorbed species refers to a zwitterionic species ($\text{NH}_3^+.\text{RCH}.\text{COO}^-$).

In the current study, we are interested in how amino acids interact with each other on silver where intermolecular interactions may be expected to dominate the formation of ordered structures rather than the strength of the bond between the amino acid and the substrate.

Experimental Section

STM and RAIRS experiments were performed in an Omicron UHV system with a base pressure of 1×10^{-10} mbar. The chamber consists of three interlinked chambers, one housing the variable temperature STM, the second being equipped for RAIRS experiments, and the third chamber which has facilities for sample cleaning and characterization (low energy electron diffraction (LEED)/auger electron spectroscopy (AES)). The Ag{110} sample

* To whom correspondence should be addressed. E-mail: cjb14@st-and.ac.uk.

(1) Barlow, S. M.; Kitching, K. J.; Haq, S.; Richardson, N. V. *Surf. Sci.* **1998**, *401*, 322.

(2) Booth, N. A.; Woodruff, D. P.; Schaff, O.; Giessel, T.; Lindsay, R.; Baumgartel, P.; Bradshaw, A. M. *Surf. Sci.* **1998**, *397*, 258.

(3) Chen, Q.; Frankel, D. J.; Richardson, N. V. *Surf. Sci.* **2002**, *497*, 37.

(4) Efstathiou, V.; Woodruff, D. P. *Surf. Sci.* **2003**, *531*, 304.

(5) Ge, S. P.; Zhao, X. Y.; Gai, Z.; Zhao, R. G.; Yang, W. S. *Chin. Phys.* **2002**, *11*, 839.

(6) Hasselstrom, J.; Karis, O.; Weinelt, M.; Wassdahl, N.; Nilsson, A.; Nyberg, M.; Pettersson, L. G. M.; Samant, M. G.; Stohr, J. *Surf. Sci.* **1998**, *407*, 221.

(7) Kang, J. H.; Toomes, R. L.; Polcik, M.; Kittel, M.; Hoeft, J. T.; Efstathiou, V.; Woodruff, D. P.; Bradshaw, A. M. *J. Chem. Phys.* **2003**, *118*, 6059.

(8) Nyberg, M.; Hasselstrom, J.; Karis, O.; Wassdahl, N.; Weinelt, M.; Nilsson, A.; Pettersson, L. G. M. *J. Chem. Phys.* **2000**, *112*, 5420.

(9) Nyberg, M.; Odellius, M.; Nilsson, A.; Pettersson, L. G. M. *J. Chem. Phys.* **2003**, *119*, 12577.

(10) Rankin, R. B.; Sholl, D. S. *Surf. Sci.* **2004**, *548*, 301.

(11) Toomes, R. L.; Kang, J. H.; Woodruff, D. P.; Polcik, M.; Kittel, M.; Hoeft, J. T. *Surf. Sci.* **2003**, *522*, L9.

(12) Zhao, X. Y.; Gai, Z.; Zhao, R. G.; Yang, W. S. *Acta Phys. Sinica* **1999**, *48*, 94.

(13) Zhao, X. Y.; Yan, H.; Zhao, R. G.; Yang, W. S. *Langmuir* **2003**, *19*, 809.

(14) Williams, J.; Haq, S.; Raval, R. *Surf. Sci.* **1996**, *368*, 303.

(15) Zhao, X. Y.; Zhao, R. G.; Yang, W. S. *Surf. Sci.* **1999**, *442*, L995.

(16) Wang, H.; Zhao, X. Y.; Zhao, R. G.; Yang, W. S. *Chin. Phys. Lett.* **2001**, *18*, 445.

(17) Zhao, X. Y. *J. Am. Chem. Soc.* **2000**, *122*, 12584.

(18) Zhao, X. Y.; Zhao, R. G.; Yang, W. S. *Langmuir* **2000**, *16*, 9812.

(19) Wang, H.; Zhao, X. Y.; Yang, W. S. *Acta Phys. Sinica* **2000**, *49*, 1316.

(20) Chen, Q.; Frankel, D. J.; Richardson, N. V. *Langmuir* **2001**, *17*, 8276.

(21) Stewart, S.; Fredericks, P. M. *Spectrochim. Acta Part A* **1999**, *55*, 1641.

(22) Zhao, X. Y.; Yan, H.; Tu, X. W.; Zhao, R. G.; Yang, W. S. *Langmuir* **2003**, *19*, 5542.

(23) Zhao, X. Y.; Yan, H.; Zhao, R. G.; Yang, W. S. *Langmuir* **2002**, *18*, 3910.

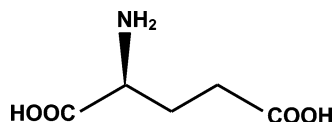


Figure 1. Schematic diagram showing the molecular structure of (S)-glutamic acid.

was first cleaned by cycles of Ar⁺ bombardment (1.0 kV) and annealing to 700 K until no impurities could be detected by AES and a sharp (1 × 1) LEED pattern was observed. The sample was transferred under UHV into the RAIRS chamber. A background spectrum was taken and then the sample was exposed to (S)-glutamic acid ((S)-GA), sublimed from a differentially pumped and baked solid doser. RAIRS data were taken as functions of exposure to (S)-GA and of sample temperature in the range 300–375 K. A Nicolet Nexus 860 FTIR spectrometer was used to acquire RAIRS data using a mercury cadmium telluride detector cooled by liquid nitrogen. After completion of the RAIRS experiment, the sample was transferred to the STM chamber where images were taken at room temperature. STM measurements were made with a chemically etched W tip in constant current mode.

Results and Discussion

To ascertain the molecular conformation of (S)-GA on Ag{110}, it is important to consider the various possible adsorption modes of the molecule. At room temperature and atmospheric pressure, (S)-GA (Figure 1) is a white solid which, like other amino acids, exists in the zwitterionic form, HOOC·CH₂·CH₂·NH₃⁺·CH₂·COO⁻.²⁴ The crystal structures of (S)-GA have been characterized for two polymorphs, alpha²⁵ and beta.²⁶ Each of these structures has a tetragonal unit cell. Adjacent glutamic acid molecules are linked together via N–H...O hydrogen bonds between the –NH₃⁺ group and the carboxylate group and by H-bonding interactions between the carboxylate group and the aliphatic –COOH group. The unit cell of the alpha polymorph is close to cubic (7.1 × 8.3 × 10.3 Å³). The unit cell of the beta polymorph has a more elongated shape (5.2 × 6.9 × 17.3 Å³). In the gas phase, the most stable conformer is thought to be the nonzwitterionic form.²⁷

Our analysis of the vibrational spectra for adsorbed glutamic acid is greatly helped by reference to two theoretical papers by Ramirez and co-workers.^{24,27} In these manuscripts, the vibrational spectra for isolated (S)-GA molecules in the zwitterionic²⁴ and nonzwitterionic²⁷ forms were calculated and, in the latter case, measured by IR matrix spectroscopy.

Ag{110}-(S)-Glutamic Acid 300 K (RAIRS/STM). Figure 2 shows the RAIR spectra as a function of increasing exposure to (S)-glutamic acid at 300 K. At low exposure, the spectrum is dominated by bands at 2946, 1651, 1574, and 1387 cm⁻¹ with an additional weak band at 1462 cm⁻¹. As coverage increases, a series of new bands are observed in the 1200–1500 cm⁻¹ range, the 1651 cm⁻¹ gradually disappears, and two intense carbonyl bands emerge at 1692 and 1723 cm⁻¹.

Lopez Navarette et al.²⁷ used IR matrix spectroscopy and DFT calculations to investigate the IR spectrum of nonzwitterionic (S)-glutamic acid. They showed that the two C=O groups in the free molecule have vibrational stretching frequencies at 1781 and 1754 cm⁻¹. By contrast, the zwitterionic form of (S)-glutamic acid exhibits a single

carbonyl stretching frequency at 1659 cm⁻¹.²⁴ In our experiments, we never observed carbonyl bands at higher frequencies than 1723 cm⁻¹. Such bands are compatible with GA in the anionic form but imply that the carbonyl groups are involved either in intermolecular interactions or in direct interactions with the Ag substrate which cause a downshifting of the vibrational frequency of the ν(C=O) bands. At low (S)-glutamic acid exposure, we only observe one band in the 1650–1800 cm⁻¹ range. This leads us to conclude that one carbonyl group remains intact, while the other acid group undergoes deprotonation to form a carboxylate species. Since the pK_A of the amino acid COOH group is considerably lower than that of the aliphatic acid group in (S)-glutamic acid, one can assume that the deprotonation involves the amino acid moiety. The band at 1651 cm⁻¹, which is very similar in frequency to the ν(C=O) band of the zwitterionic form,²⁴ may be explained as a carbonyl band strongly downshifted either by inter- or intramolecular interactions. It may be that, at low coverage, the zwitterionic species is favored, as has been observed for (S)-glutamic acid on Ni{111}.²⁸ However, the band in our spectra at 1574 cm⁻¹ can be assigned to the scissor mode of the NH₂ group with the N atom interacting directly with the surface. A band with similar vibrational frequency has been observed for other amino acids on Cu{110}^{1,14} and also for (S)-glutamic acid on Ni{111} at relatively high coverage.²⁸ This assignment suggests that under these conditions the dominant adsorbed species is anionic glutamate, in contrast to the conclusions drawn by Stewart and Fredericks.²¹ The band at 1387 cm⁻¹ is likely to be the symmetric stretching frequency of the carboxylate of the amino acid functionality. The lack of bands due to the asymmetric stretching modes of the carboxylate functionality points to the two oxygen atoms of the OCO group being approximately equidistant from the Ag{110} surface by application of the IR metal–surface selection rule. In such a geometry, the dynamic dipole moment of the asymmetric mode would be parallel to the {110} plane. Other amino acids on Cu{110} are thought to bind via the carboxylate and NH₂ functionalities across the {110} troughs (e.g., glycine²). The weak intensity of the ν_s(OCO) group of (S)-alanine²⁹ compared to formate on Cu{110}³⁰ has been explained by the plane of the OCO bond of alanine describing an acute angle with the {110} plane of the substrate. Since the spacing across the {110} troughs for Ag is 12.7% expanded compared to Cu, the amino acid functionality would be expected to adopt an even more parallel geometry in the case of Ag. Even at the highest coverages, Figure 2 reveals that the intensity of the ν(OCO) band never exceeds 0.15%, supporting this argument. The adsorption mode of the amino acid functionality may be expected to be quite similar to that observed on Cu. Casarin et al.³¹ reported a theoretical study of the adsorption of formate on Ag{110} which concluded that the carboxylate adsorbs most favorably in the bidentate bichelate geometry analogous to the adsorption site for formate on Cu{110}.^{30,32–34}

(28) Jones, T. E.; Urquhart, M. E.; Baddeley, C. J. *Surf. Sci.* **2005**, *587*, 69.

(29) Barlow, S. M.; Louafi, S.; Le Roux, D.; Williams, J.; Muryn, C.; Haq, S.; Raval, R. *Langmuir* **2004**, *20*, 7171.

(30) Hayden, B. E.; Prince, K.; Woodruff, D. P.; Bradshaw, A. M. *Surf. Sci.* **1983**, *133*, 589.

(31) Casarin, M.; Maccato, C.; Vittadini, A. *J. Chem. Soc., Faraday Trans.* **1998**, *94*, 797.

(32) Crapper, M. D.; Riley, C. E.; Woodruff, D. P. *Surf. Sci.* **1987**, *184*, 121.

(33) Crapper, M. D.; Riley, C. E.; Woodruff, D. P.; Puschmann, A.; Haase, J. *Surf. Sci.* **1986**, *171*, 1.

(34) Hayden, B. E.; Prince, K.; Woodruff, D. P.; Bradshaw, A. M. *Vacuum* **1983**, *33*, 876.

(24) Ramirez, F. J.; Navarrete, J. T. L. *Spectrochim. Acta Part A* **1995**, *51*, 293.

(25) Lehmann, M. S.; Nunes, A. C. *Acta Crystallogr., Section B* **1980**, *36*, 1621.

(26) Hirokawa, S. *Acta Crystallogr.* **1955**, *8*, 637.

(27) Navarrete, J. T. L.; Bencivenni, L.; Ramondo, F.; Hernandez, V.; Ramirez, F. J. *J. Mol. Struct. (THEOCHEM)* **1995**, *330*, 261.

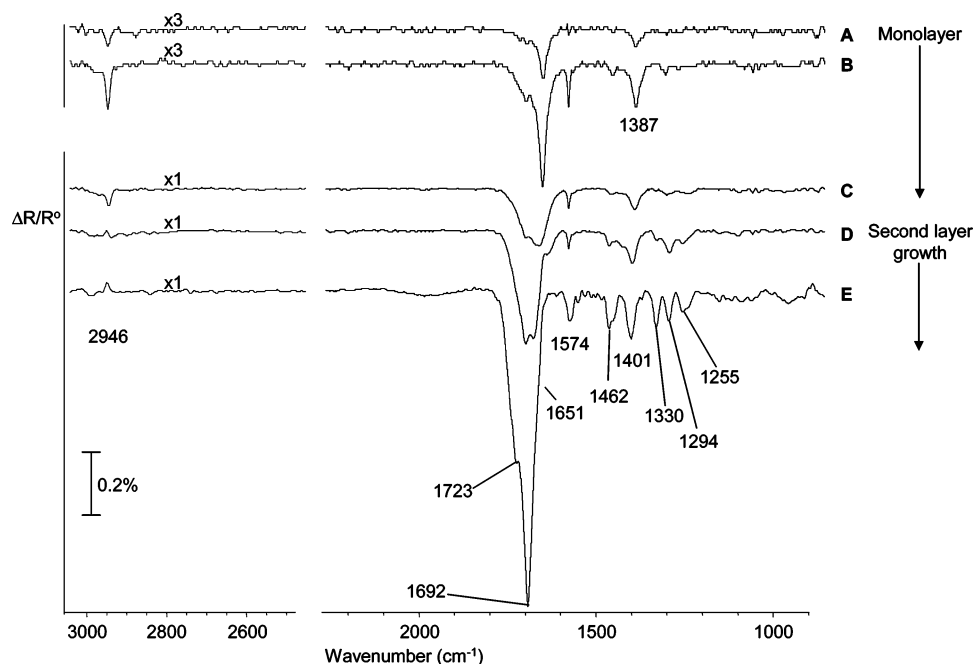


Figure 2. RAIRS spectra following the adsorption of (S)-glutamic acid on Ag{110} at 300 K as a function of (S)-glutamic acid exposure. The temperature of the (S)-glutamic acid solid doser was 400 K.

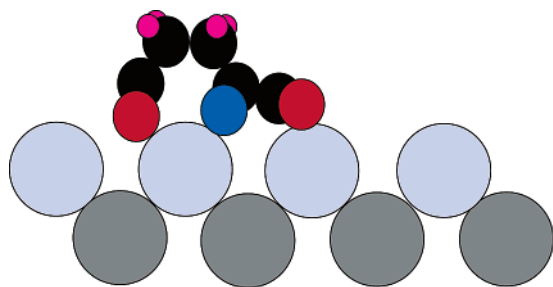


Figure 3. Proposed adsorption geometry for the glutamate species present in the $\langle 4\ 2\ |\ -1\ 5 \rangle$ structure.

The 2946 cm^{-1} band is assignable to the $\nu_s(\text{CH}_2)$ mode of the methylene groups in (S)-glutamic acid. The appearance of this band and the absence of the $\nu_{as}(\text{CH}_2)$ band gives information on the geometry of the $(\text{CH}_2)_2$ backbone of the molecule at low coverage. By application of the surface dipole selection rule, we conclude that the C–C bond is approximately parallel to the surface with the two sets of H atoms pointing away from the surface. This is supported by the fact that the scissors mode of the CH_2 group (1462 cm^{-1}) is observed at this coverage (albeit weakly). This mode has the same symmetry as the $\nu_s(\text{CH}_2)$ mode.

On the basis of the above, we are able to conclude a geometry for the low coverage (S)-glutamic acid species as shown in Figure 3.

At high coverage, extra bands are observed including the CH_2 wagging mode at 1330 cm^{-1} . In addition, the 1462 cm^{-1} band (CH_2 scissor mode) increases in intensity. The observation of the wagging mode indicates a change of the (S)-GA adsorption geometry which will be discussed in more detail later on.

Following the adsorption of (S)-glutamic acid on Ag{110}, we observed at least three distinct ordered molecular adlayers.

Adlayer Structure 1, the $\langle 4\ 2\ |\ -1\ 5 \rangle$ Phase. STM experiments revealed that at low exposure (corresponding to spectra (A) and (B) in Figure 2) two distinct surface morphological features are observed, as demonstrated in

Figure 4a. Much of the surface is covered by 1-D features parallel to the $[-110]$ surface direction. These facets are similar to those observed for uracil on Cu{110}³⁵ and glycine on Au{110}- (1×2) ²³ which may be ascribed to 1-D faceting of the surface. We were unable to identify any molecular features in these regions. Similar observations were made by Zhao and co-workers for amino acids on Cu surfaces. They described this behavior as being like that of a 2-D gas, extremely efficient molecular diffusion accounting for the lack of molecular features in the STM images.³⁶ Between the faceted regions of the surface, we observed “flatter” regions. Imaging in these regions, we observed ordered molecular features (Figure 4b). The molecular order increased dramatically on annealing to 375 K (Figure 4, panels c and d) though the overall periodicity remained the same. Because the periodicity remains the same, we shall assume that the molecular geometry is also unchanged upon annealing. The LEED pattern and the STM images are consistent with a unit cell described in matrix notation as $\langle 4\ 2\ |\ -1\ 5 \rangle$. The most obvious features in the STM images of Figure 4, panels c and d, are the periodic dark holes in the structure. Each hole is surrounded by four bright features, the positions of which are very well-defined throughout the image. In addition, a less intense feature lies directly between each pair of bright features along the $\langle 4,2 \rangle$ direction. If four of these bright features describe the corners of the adlayer unit cell as shown in Figure 4d, it can be seen that the center of the unit cell contains additional features running along the $\langle 4,2 \rangle$ direction whose periodicity is less well-defined even after the 375 K annealing treatment. A schematic diagram illustrating the relationship between the adlayer molecules and the underlying Ag{110} lattice is shown in Figure 4e. We believe that the corners of the unit cell consist of anionic (S)-glutamate species separated by a $\langle 4,2 \rangle$ vector. Directly between these two species is found another (S)-glutamate species. Since the position of this species can be described by a $\langle 2,1 \rangle$ vector with respect to the corner species, we believe that this species has a

(35) Frankel, D. J.; Chen, Q.; Richardson, N. V. Unpublished work.

(36) Zhao, X. Y.; Wang, H.; Yan, H.; Gai, Z.; Zhao, R. G.; Yang, W. *S. Chin. Phys.* **2001**, *10*, S84.

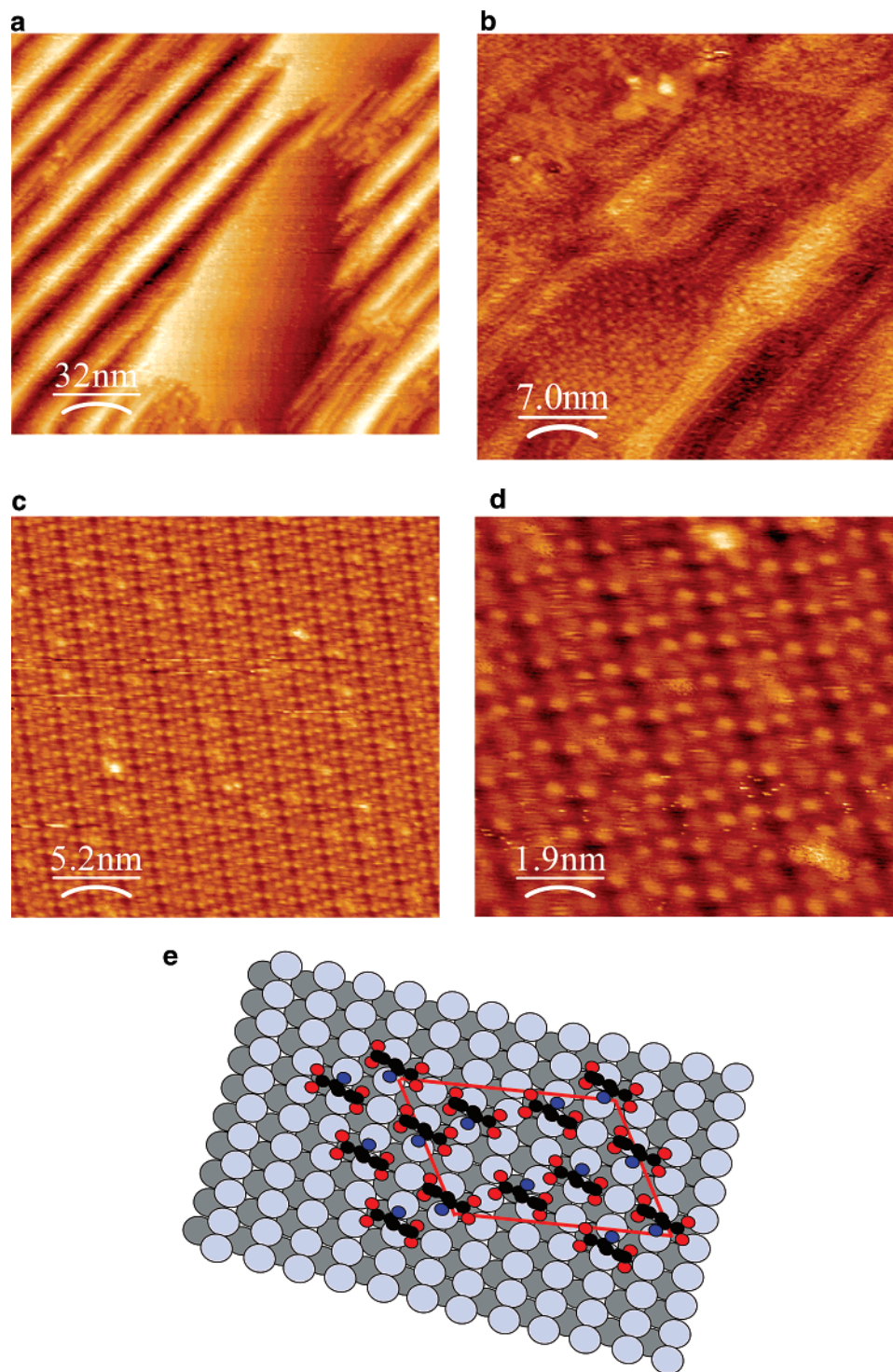


Figure 4. STM images showing (a) the coexistence of the 1-D facets and the $\langle 4\ 2|-1\ 5 \rangle$ phase produced at low (S)-glutamic acid coverage at 300 K (-0.55 V; 0.16 nA), (b) the $\langle 4\ 2|-1\ 5 \rangle$ phase formed at 300 K (-0.71 V; 0.44 nA) and following an anneal to 375 K, (c and d) (-0.55 V; 0.16 nA). (e) Schematic diagram showing a proposed molecular structure for the $\langle 4\ 2|-1\ 5 \rangle$ phase

similar orientation and adsorption site to the corner species. Approximately one-third of the distance along the $\langle -1,5 \rangle$ direction can be found an (S)-glutamate species. We believe that this species is rotated by 180° compared to the corner species facilitating intermolecular H-bonding between the aliphatic $-\text{COOH}$ group and the $-\text{NH}_2$ group of the neighboring molecule. We propose that the remaining two molecules in the unit cell, whose positions are less well-defined, are not involved in this H-bonded network. Our model proposes that the total number of molecules per unit cell is six giving a coverage of $6/22$ or 0.27 ML. The average area occupied by 1 molecule in this structure

is $43.0\ \text{\AA}^2$. This compares with $27.7\ \text{\AA}^2$ for the (3×2) structure adopted by glycine¹ and alanine¹⁴ on Cu{110}. This difference in size is anticipated since (S)-glutamic acid is relatively large in comparison with glycine or alanine.

It should be stressed that the $\langle 4\ 2|-1\ 5 \rangle$ structure covers only a small fraction of the Ag{110} surface. Since the RARS bands are relatively weak under the experimental conditions where this structure is observed, one may conclude that the remainder of the surface which exhibits the extended 1-D features contains very few adsorbed (S)-glutamic acid molecules.

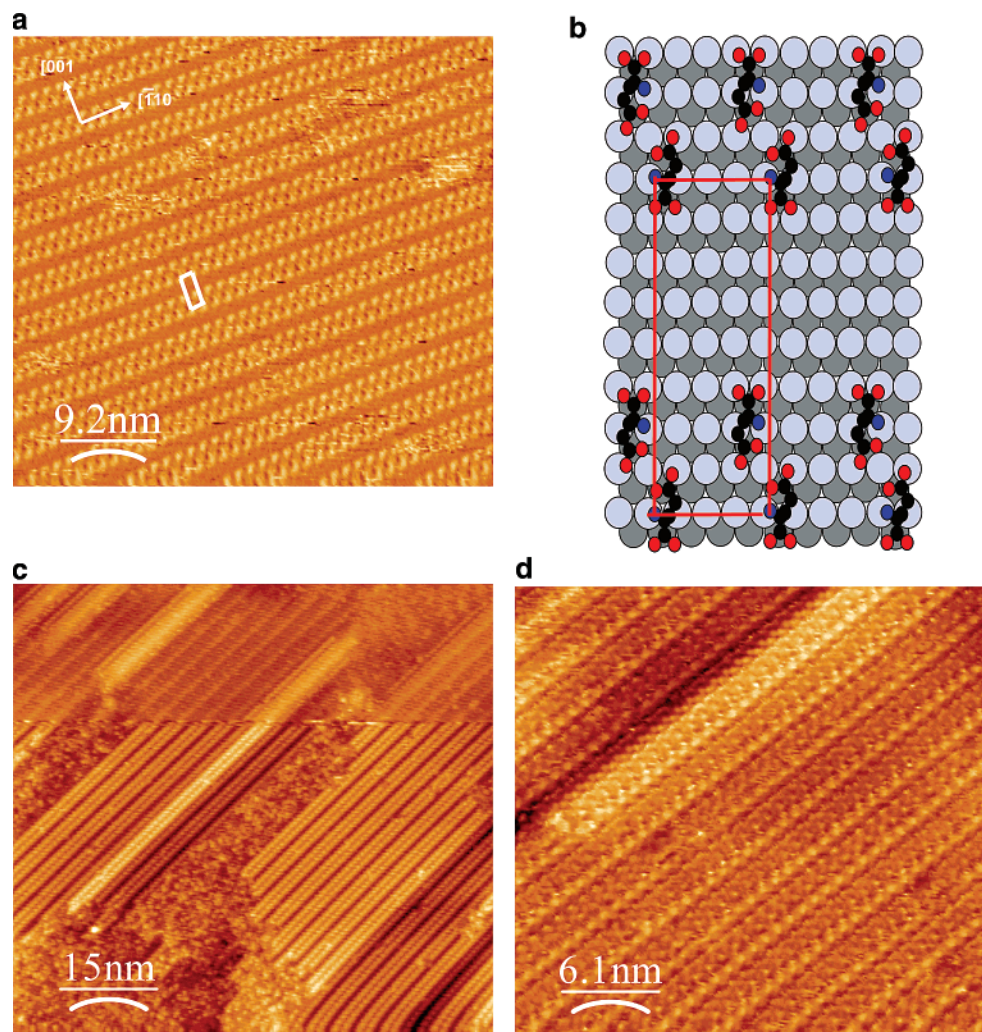


Figure 5. (a) STM image showing the (4×8) phase of (S)-glutamic acid on Ag{110} following adsorption at 300 K (0.67 V; 0.13 nA). (b) Schematic diagram showing the proposed molecular arrangement in the (4×8) adlayer. (c) STM image showing the $c(4 \times 12)$ structure produced by a high (S)-glutamic acid exposure annealed to 423 K (−0.65 V; 0.16 nA). (d) STM image showing $c(4 \times 12)$ structure imaged under different tip condition (−0.65 V; 0.16 nA).

Adlayer Structure 2, the $(4 \times n)$ Phase. As the exposure is increased, the rapid growth of the CH_2 scissor mode at 1462 cm^{-1} and the CH_2 wagging mode at 1330 cm^{-1} , indicate a change in geometry of the methylene units of (S)-glutamic acid (see spectra D and E in Figure 2). Similarly, the $\text{C}=\text{O}$ stretching frequency of the aliphatic COOH group shifts up and the $\nu_s(\text{OCO})$ band of the amino acid carboxylate group shifts to higher frequency (1401 from 1387 cm^{-1}). In STM, at intermediate coverages (corresponding to spectrum C in Figure 2), the ordered structure shown in Figure 5a is observed. This can best be explained by dimers of (S)-glutamic acid adopting geometries shown schematically in Figure 5b. The formation of $\text{O}-\text{H}\cdots\text{O}$ bonds between adjacent aliphatic COOH groups would cause a reorientation of the methylene units and may cause a slight change in the geometry of the amino acid functionality. A $p(4 \times 8)$ LEED pattern is observed for this structure. If each feature in the STM image corresponds to one molecule, this gives a local coverage of $1/16$ or 0.063 ML . Given the relatively small footprint of an (S)-glutamic acid molecule (maximum length $\sim 8\text{ \AA}$), a remarkably large 32.6 \AA periodicity exists in the $[001]$ direction. It is possible that the large distance between adjacent rows of dimers is caused by electrostatic repulsions between the negatively charged carboxylate groups of adjacent (S)-glutamate species. Moreover we note that the local coverage is significantly lower than

the one observed in the low exposure case. This apparent contradiction is explained by considering that the $\langle 4\ 2|-1\ 5 \rangle$ structure covers only a small part of the surface, as indicated by the small intensity in IR spectra, whereas the $p(4 \times 8)$ phase extends to a larger area. It is also possible that molecules exist between the dimer rows but are too mobile at 300 K to be imaged with STM.

At higher exposure, a LEED pattern consistent with a $c(4 \times 12)$ structure is observed once the sample has been annealed in the range 375–475 K. The STM images of this phase are highly complex. The STM images pick out both $c(4 \times 12)$ and $p(4 \times 6)$ periodicities depending on the relative positions of the dimers in adjacent rows. For example, in the lower half of Figure 5c, it appears that there are rows of dimers similar to those observed in the $p(4 \times 8)$ structure though with an apparent periodicity of 24.4 \AA in the $[001]$ direction (consistent with 6 Ag–Ag spacings). A change in the tip condition mid-scan reveals a slightly different image with the brightest feature now running along the center of the dimer rows. This is better observed in Figure 5d. Here additional features appear in the unit cell. In the $c(4 \times 12)$ unit cell, we can clearly identify six discrete features per unit cell, which would give a local coverage of 0.25 ML . It may be the case that additional molecules are contained within the unit cell which we were unable to resolve. One explanation for this behavior may be that under certain tip conditions the

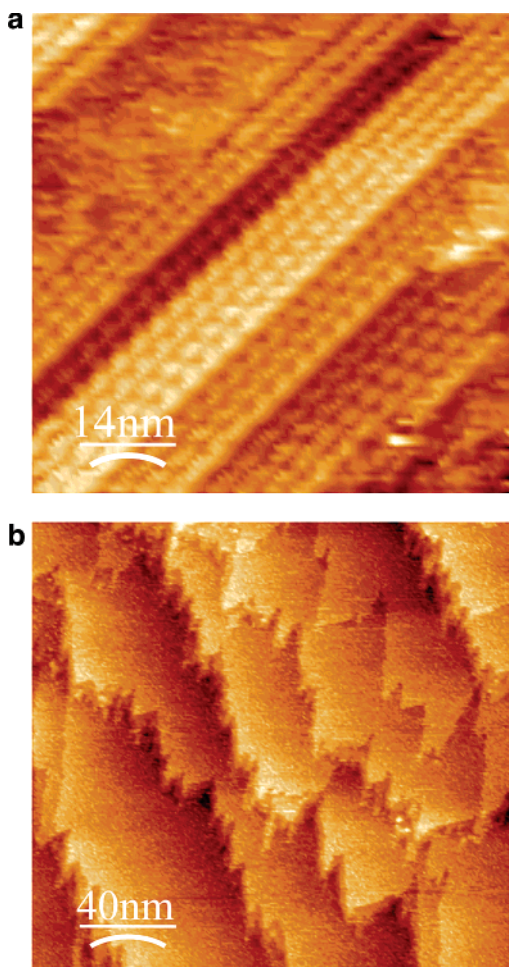


Figure 6. STM images displaying adsorbate induced faceting (a) at 425 K (−0.65 V; 0.99 nA) and (b) at 300 K (−0.69 V; 0.25 nA).

amino acid functionality is imaged as being bright, whereas under different tip conditions, the dimerized −COOH groups appears bright. It is also conceivable that Ag adatoms play a role in this structure. We know that extensive adsorbate induced faceting occurs in the Ag/(S)-glutamic acid system as evidenced by Figure 6a,b. The formation of Cu-carboxylic acid complexes has been proposed for several different systems on the low index facets of the Cu surface (e.g., trimesic acid on Cu{001}³⁷ and benzoic acid on Cu{110}).³⁸ It may be no coincidence that the (4 × *n*) structures follow the alignment of the 1-D facets observed at low (S)-glutamic acid exposure. Though we have no direct evidence to support this, it may be that the 1-D facets act as nucleation sites for the growth of the (4 × *n*) structures.

The complexity of the carbonyl stretching region of the IR spectrum increases at intermediate to high (S)-glutamic acid exposure (spectra C–E in Figure 2). This can be interpreted by the growth of a second layer (possibly several layers) of (S)-glutamic acid. When the surface is annealed to 423 K, STM reveals that the second adlayer is ordered with a periodicity defined by the monolayer. This is shown most clearly by the bright stripe in Figure 5c. The strong monolayer → second layer interaction causes the carbonyl groups for the evolving second layer to be downshifted by ~50 cm^{−1} from the positions

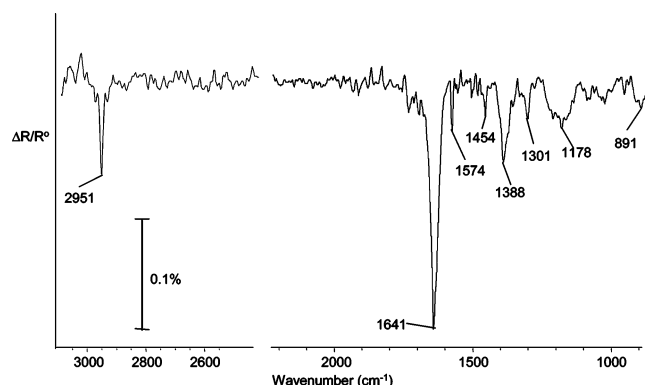


Figure 7. RAIRS spectrum following the adsorption of (S)-glutamic acid on Ag{110} at 373 K. No coverage dependence was observed in this experiment. The temperature of the (S)-glutamic acid solid doser was 400 K.

anticipated for an isolated neutral (S)-glutamic acid molecule.²⁷ It seems that the onset of second layer growth may occur considerably before the completion of the monolayer. The formation of the second layer may be kinetically limited, and we have some evidence (not shown) that the growth of (S)-glutamic acid is strongly dependent on the incident flux. Remnants of the second layer can still be observed following annealing to 423 K. The thermal stability of the second layer can probably be explained by intermolecular bonding between the aliphatic COOH group of (S)-glutamate in the monolayer and the functional groups of (S)-glutamic acid. It is difficult to determine the charge state of the amino acids adsorbed in the second layer. Chemical intuition would point to the likelihood of zwitterionic species. At 300 K, we were unable to grow thermally stable multilayers of (S)-glutamic acid which would have given a clearer answer to this question.

Adsorbate Induced Faceting. After annealing to 425 K, some areas of the surfaces exhibited a highly faceted structure (Figure 6a). The periodicity of the facets in the [001] direction is ~32 Å, i.e., similar to the 8 × periodicity observed in the (4 × 8) structure. In the [−110] direction, the periodicity is ~40 Å. These data are consistent with the formation of preferred step directions along [−112] and [1−12] vectors. The phenomenon of adsorbate induced faceting and step-bunching is related to the stabilization of certain facets by the adsorbate.³⁹ There is thought to be a strong correlation between the direction of the periodicity in the molecular adlayer and the facet induced by the adsorbate.¹⁷ In this case, we do not have any molecularly resolved images on the facets. However, the triangular nature of the facets is strikingly similar to the triangular arrangements of the molecular features imaged in the (4 × 8) and c(4 × 12) structures (Figure 4). When the adsorbate is chiral, it has been observed that the facets produced are themselves chiral, for example, lysine on Cu{100}.¹⁷ Although there is no evidence for the formation of chiral facets in the image displayed in Figure 6a, there is a pronounced asymmetry in the facets observed in Figure 6b produced by (S)-glutamic acid adsorption at 300 K. This is a region of the surface where the step edges run parallel to the [001] direction (in contrast to Figure 6a where the steps run parallel to the [−110] direction). Two types of facet are produced related by mirror symmetry with the mirror plane defined by the [−110] surface azimuthal direction. There appears to be a much stronger tendency for facets to be produced running down the image compared to those produced in the mirror equivalent

(37) Barth, J. V.; Weckesser, J.; Lin, N.; Dmitriev, A.; Kern, K. *Appl. Phys. A* **2003**, *76*, 645.

(38) Chen, Q.; Perry, C. C.; Frederick, B. G.; Murray, P. W.; Haq, S.; Richardson, N. V. *Surf. Sci.* **2000**, *446*, 63.

(39) Chen, Q.; Richardson, N. V. *Prog. Surf. Sci.* **2003**, *73*, 59.

Table 1. Vibrational Assignments of Absorption Bands (in cm^{-1}) of Adsorbed (S)-GA by Comparison with Analogous Adsorbed Species and Gas Phase (S)-GA

assignment	300 K		373 K	zwitterion ²⁴	nonzwitterion ²⁷	(S)-Ala/Cu{110} ¹⁴
	monolayer	second layer				
$\nu_{\text{sym}}(\text{CH}_2)$	2946	2946	2951	2967	2965	
$\nu(\text{C}=\text{O})^{\text{acid}}$		1723			1781	
$\nu(\text{C}=\text{O})^{\text{acid}}$	1651	1692	1631		1754	
$\nu(\text{C}=\text{O})^{\text{acid}}$				1659		
$\delta_{\text{asym}}(\text{NH}_3^+)$				1641, 1631, 1615		
$\delta_{\text{asym}}(\text{NH}_2)$	1574	1574	1575		1635	1576
$\nu_{\text{sym}}(\text{NH}_3^+)$				1516		
$\delta(\text{CH}_2)$	1462	1462	1454	1438	1405	
$\nu_{\text{sym}}(\text{OCO}^-)$	1387	1401	1388	1421		1415
$\omega(\text{CH}_2)$		1330		1259	1337	
$\omega(\text{CH}_2), \delta(\text{CH}), \text{r}(\text{NH}_3^+)$				1312		
$\text{t}(\text{CH}_2), \delta_{\text{asym}}(\text{NH}_2)$		1294	1301		1279	
$\nu(\text{CN})$		1255			1234	
$\text{t}(\text{CH}_2), \nu(\text{CN})$			1178		1139	
$\nu(\text{CC})$				1056	1092	
$\nu(\text{CC}), \text{r}(\text{CH}_2)$				920	1024	
$\nu(\text{CC}), \nu(\text{CO})$			891	866	886	

azimuthal direction of the clean surface. On Cu, faceting is normally observed following an annealing treatment.³⁹ In the case of Ag, a lower faceting temperature may be expected in view of the greater mobility of surface Ag atoms at 300 K. Although the experiment of Figure 6b suggests the observation of a chiral effect, it should be pointed out that more experiments are required to determine the

statistical distribution of such chiral facets. It is known that a slight offcut of the crystal can result in the metal surface itself being intrinsically chiral.

Ag{110}-(S)-Glutamic Acid, $T = 373$ K (RAIRS/STM). *Adlayer Structure 3, the $\langle 3\ 2\ |\ -3\ 3 \rangle$ Phase.* Figure 7 shows a RAIRS spectrum recorded after a long (S)-glutamic acid exposure at $T = 373$ K. It is very similar to that achieved for low coverage (S)-glutamic acid adsorption at 300 K. However, STM (Figure 8a) reveals that deposition at 373 K gives a markedly different adsorbate structure to that observed following adsorption at 300 K and subsequent annealing (i.e., the $\langle 4\ 2\ |\ -1\ 5 \rangle$ structure). The local coverage in the $\langle 3\ 2\ |\ -3\ 3 \rangle$ structure is 2/15 or 0.133 ML (Figure 8b). There appears to be a well-defined periodicity along the [001] direction. In the $[-110]$ direction, the ordering is more complex. There is an additional superstructure with a periodicity of ~ 60 Å with the 2-D molecular density varying significantly. This implies that the adsorption site of (S)-glutamic acid on Ag is relatively flexible. In contrast, (R,R)-tartaric acid⁴⁰ and (S)-alanine²⁹ on Cu{110} exhibit structures with well-defined channels between small clusters of molecules. In these cases, it is thought that the interaction between the adsorbate and the Cu substrate is the dominant factor in the formation of the overlayer. In the case of Ag, it appears that the adsorbate–molecule and molecule–molecule interactions are of a similar strength. In the molecular arrangement shown in Figure 8b (consistent with the LEED pattern), the intermolecular separation is too large for the formation of significant intermolecular H-bonds. This corresponds to the regions of low molecular packing density in the STM image. However, in the more dense regions of the structure, it is likely that relatively strong intermolecular H bonds can occur.

Conclusions

1. In contrast with previous SERS studies,²¹ (S)-glutamic acid adsorption on Ag{110} in the range 300–375 K occurs predominantly in the anionic form.

2. Several different ordered structures are produced at different adsorption temperatures and adlayer coverages.

3. There are subtle differences between the nature of the adlayers produced on Ag{110} compared to those formed by similar molecules on Cu{110}. This is thought

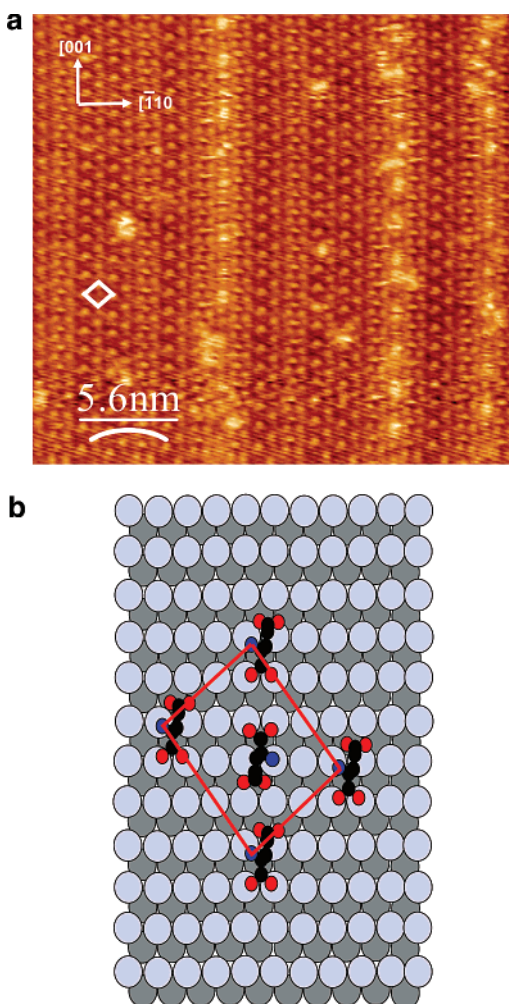


Figure 8. (a) STM image showing the $\langle 3\ 2\ |\ -3\ 3 \rangle$ phase of (S)-glutamic acid on Ag{110} following adsorption at 373 K (-0.5 V; 0.19 nA). (b) Schematic diagram showing the proposed molecular arrangement in the $\langle 3\ 2\ |\ -3\ 3 \rangle$ adlayer.

(40) Lorenzo, M. O.; Haq, S.; Bertrams, T.; Murray, P.; Raval, R.; Baddeley, C. J. *J. Phys. Chem. B* **1999**, *103*, 10661.

to derive from the weaker molecule-surface interaction which makes the adsorption site of (S)-glutamic acid more flexible.

4. Adsorbate induced faceting is observed upon glutamic acid exposure. A better statistical analysis is however required to determine to what extent, if at all, chiral faceting is observed.

Acknowledgment. This project was funded by a CRUI-British Council partnership. In addition, we are grateful to EPSRC for funding a PDRA for T.E.J. (GR/R16198/01). We are grateful to Professor Neville Richardson for the use of his STM/RAIRS chamber.

LA050414B